INTERFERENCE CANCELLATION USING ARTM TIER-1 WAVEFORMS IN AERONAUTICAL TELEMETRY

Tariq M Ali, Mohammad Saquib
Dept. Electrical Engineering, University of Texas at Dallas, Richardson, TX

Michael Rice
Dept. Electrical & Computer Engineering, Brigham Young University, Provo, UT

ABSTRACT

This paper describes and interference cancellation technique appropriate for ARTM Tier-1 waveforms. The technique requires the estimators for the bit sequences for the adjacent channels as well as the power levels of the adjacent channels. Simulation results show that the interference canceller allows a more dense "channel packing" thereby creating a channel utilization 67% ~ 100% greater than the current IRIG 106 recommendations.

KEY WORDS

adjacent channel interference, interference cancellation, FQPSK, SOQPSK

INTRODUCTION

As the complexity and sophistication of systems to be tested has increased, the bit rates required for the telemetry downlink have also increased. This has created tremendous pressure on the spectrum allocations to aeronautical telemetry in the L and S-bands. Spectrum reallocations in 1997 of 50 MHz in the upper S-band *from* telemetry *to* other applications prompted the search for more bandwidth efficient modulations for use in aeronautical telemetry in the late 1990s [1]. In 2000, Feher-patented QPSK (FQPSK) [2] was adopted as a choice in the IRIG 106 standard. Later, Shaped Offset QPSK (SOQPSK) [3] and a variant of FQPSK, known as FQPSK-JR [4]-[5], were adopted as interoperable alternatives in 2004. These waveforms, known collectively as "ARTM Tier-1 waveforms," were chosen since they have twice the spectral efficiency of PCM/FM, even when used with non-linear power amplifiers [6].

The central motivation in selecting the new waveforms was to use the remaining telemetry spectrum allocations more efficiently. An important factor in efficient spectrum utilization is channel spacing (i.e. the frequency difference between the carrier frequencies of adjacent channels). The limiting factor in channel spacing assignments is a phenomenon known as adjacent channel interference (ACI) [7]. An illustration of adjacent channel interference and how it might limit channel spacing is illustrated in Figure 1. Shown are the spectra of three telemetry signals. The spectrum centered at frequency f_0 is the desired signal. In this example, the next

frequency assignment below the desired signal is a lower bit rate signal assigned a carrier frequency f_1. The next frequency assignment above the desired signal is a telemetry signal with the same bandwidth assigned to a carrier frequency f_2. The carrier separations, $\Delta f_1 = f_0 - f_1$ and $\Delta f_2 = f_2 - f_0$, and the relative powers ΔP_1 and ΔP_2, determine the degree by which the adjacent signals interfere with the desired signal.

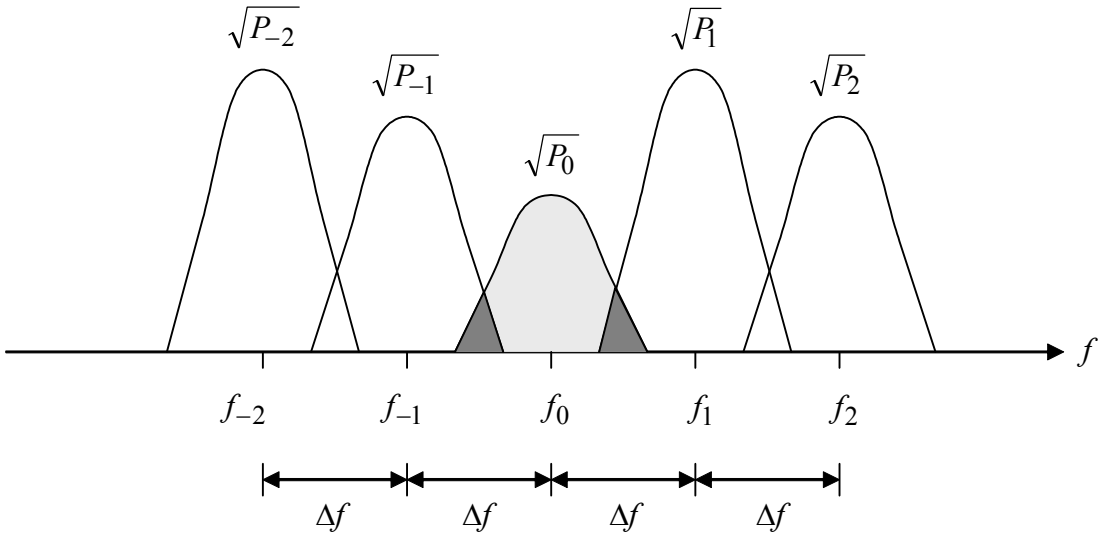

Figure 1: An illustration of adjacent channel interference.

Efficient spectral usage requires the assigned carriers to be as closely spaced as possible (i.e., Δf_1 and Δf_2 must be as small as possible). As the carriers are moved closer to each other, the spectra overlap thereby introducing an interference signal into the demodulator and detection circuitry tuned to the desired signal centered at f_0. Laboratory experiments measuring bit error rate penalties as a function of channel spacing, bit rate, modulation type, carrier to interference ratio (C/I), and receiver design were performed by Eugene Law [8] – [10]. The end result was a formula for channel spacing suitable for use by range frequency managers in carrier frequency assignments. Haghdad and Feher investigated the effect of *co-channel interference* on FQPSK-B by measuring the increase in bit error rate in the presence of an in-band sinusoid [11].

To date little work has been done on interference canceling techniques suitable for use with ARTM Tier-1 waveforms in a telemetry setting. Law noted that the undesirable effects of strong adjacent channel interference can sometimes be mitigated by proper selection of the IF filter when PCM/FM with limiter/discriminator detection is used or with ARTM Tier-1 waveforms when strong interferers present dynamic range problems in the receiver architecture [8] – [10]. Relying solely on the IF filter for ACI mitigation would require an infinitely adjustable filter. Haghdad and Feher noted that the use non-linear amplification at the receiver tends to suppress a narrow-band interferer [11]. However the benefits of this technique do not generalize to the scenario presented in Figure 1.

In this paper, we demonstrate that interference cancellation can reduce the channel spacing required to maintain a reliable communications link. These techniques use sophisticated signal processing techniques and are intended for use with a sampled-data receiver as illustrated in

Figure 2. We show that using these techniques allows multiple telemetry users to be packed closer together in the allocated frequency bands thus improving the overall efficiency with which the telemetry spectrum allocations are used. This benefit comes at the cost of complexity: the computational burden required by the interference cancellers increase the complexity of the demodulator. However, this complexity resides on the ground where size, weight, and space are less important.

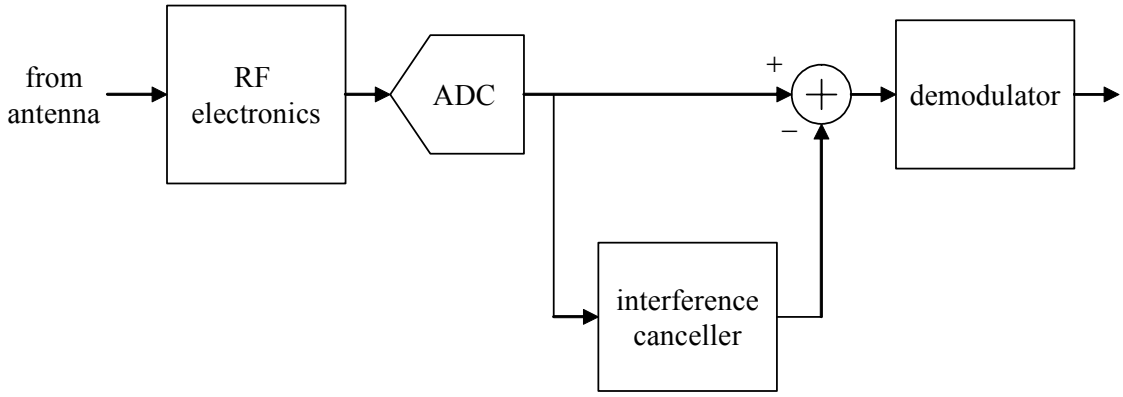

Figure 2: Structure of sampled data receiver illustrating the functional role of the interference canceller.

ALGORITHM DEVELOPMENT

We develop an interference suppression technique for the case where an FQPSK signal is interfered by two adjacent channels, one on each side of the spectrum. The adjacent channels also carry FQPSK modulated signals. The carrier spacing is equal on both sides. As we will point out later, the same procedure can be generalized for other modulation methods as well.

Let $s(t;\mathbf{b})$ be the complex baseband representation of an FQPSK signal generated by the bit sequence $\mathbf{b}$ and let $S(f;\mathbf{b})$ be the Fourier transform of $s(t;\mathbf{b})$. Consider the case of five signals organized as illustrated in Figure 1 where $f_0 = 0$ for convenience. We denote by $s_0(t)$ the middle signal whose spectrum is centered at $f_0 = 0$. These five signals, along with their Fourier transforms may be expressed in terms of the baseband FQPSK signal as

$$\begin{aligned}
s_{-2}(t) &= s(t;\mathbf{b}_{-2})e^{-j4\pi\Delta ft} & S_{-2}(f) &= S(f+2\Delta f;\mathbf{b}_{-2}) \\
s_{-1}(t) &= s(t;\mathbf{b}_{-1})e^{-j2\pi\Delta ft} & S_{-1}(f) &= S(f+\Delta f;\mathbf{b}_{-1}) \\
s_0(t) &= s(t;\mathbf{b}_0) & S_0(f) &= S(f;\mathbf{b}_0) \\
s_1(t) &= s(t;\mathbf{b}_1)e^{j2\pi\Delta ft} & S_1(f) &= S(f-\Delta f;\mathbf{b}_1) \\
s_2(t) &= s(t;\mathbf{b}_2)e^{j4\pi\Delta ft} & S_2(f) &= S(f-2\Delta f;\mathbf{b}_2)
\end{aligned} \qquad (1)$$

Although we consider interference from only one adjacent channel on each side, we are incorporating effects of the two outermost signals, $s_{-2}(t)$ and $s_2(t)$ for the reasons that will be clear shortly. The received baseband signal is

$$
\begin{aligned}
r_0(t) &= \sqrt{P_0}\, s_0(t) + \sqrt{P_{-1}}\, s_{-1}(t) + \sqrt{P_1}\, s_1(t) + w_0(t) \\
&= \sqrt{P_0}\, s(t;\mathbf{b}_0) + \sqrt{P_{-1}}\, s(t;\mathbf{b}_{-1}) e^{-j2\pi\Delta f t} + \sqrt{P_1}\, s(t;\mathbf{b}_1) e^{j2\pi\Delta f t} + w_0(t)
\end{aligned}
\tag{2}
$$

where $w(t)$ is a complex Gaussian random process with zero mean whose real and imaginary parts have power spectral density $N_0/2$ W/Hz. (This term represents the thermal noise.)

In order to perform interference cancellation, we need knowledge of powers P_{-1} and P_1. Let us now assume that these powers are known. In the next section we present a method for estimating these powers.

We put two additional demodulators tuned at the carrier frequencies $f_{-1} = f_0 - \Delta f$ and $f_1 = f_0 + \Delta f$. The received signals for these two demodulators are

$$
\begin{aligned}
r_{-1}(t) &= \sqrt{P_{-1}}\, s_{-1}(t) + \sqrt{P_{-2}}\, s_{-2}(t) + \sqrt{P_0}\, s_0(t) + w_{-1}(t) \\
&= \sqrt{P_{-1}}\, s(t;\mathbf{b}_{-1}) + \sqrt{P_{-2}}\, s(t;\mathbf{b}_{-2}) e^{-j2\pi\Delta f t} + \sqrt{P_0}\, s(t;\mathbf{b}_0) e^{j2\pi\Delta f t} + w_{-1}(t)
\end{aligned}
\tag{3}
$$

$$
\begin{aligned}
r_1(t) &= \sqrt{P_1}\, s_1(t) + \sqrt{P_0}\, s_0(t) + \sqrt{P_2}\, s_2(t) + w_1(t) \\
&= \sqrt{P_1}\, s(t;\mathbf{b}_1) + \sqrt{P_0}\, s(t;\mathbf{b}_0) e^{-j2\pi\Delta f t} + \sqrt{P_2}\, s(t;\mathbf{b}_2) e^{j4\pi\Delta f t} + w_1(t),
\end{aligned}
\tag{4}
$$

respectively, where $w_{-1}(t)$ and $w_1(t)$ represent the thermal noise contributions from the additional demodulators tuned to $f_{-1} = f_0 - \Delta f$ and $f_1 = f_0 + \Delta f$, respectively. We now try to obtain the transmitted bit sequence $\mathbf{b}_{-1}$ from $r_{-1}(t)$ and $\mathbf{b}_1$ and from $r_1(t)$. Due to interference and noise, these sequences may not be the same as the actual ones; hence our demodulated bit sequences are $\hat{\mathbf{b}}_{-1}$ and $\hat{\mathbf{b}}_1$. From $\hat{\mathbf{b}}_{-1}$ and $\hat{\mathbf{b}}_1$ we reconstruct the FQPSK signals $s(t;\hat{\mathbf{b}}_{-1})$ and $s(t;\hat{\mathbf{b}}_1)$, respectively, and denote the estimation errors as

$$
\begin{aligned}
\Delta s_{-1}(t) &= s_{-1}(t;\mathbf{b}_{-1}) - s_{-1}(t;\hat{\mathbf{b}}_{-1}) \\
\Delta s_1(t) &= s_1(t;\mathbf{b}_1) - s_1(t;\hat{\mathbf{b}}_1)
\end{aligned}
\tag{5}
$$

Now we perform appropriate frequency shifts on these reproduced signals corresponding to channels centered at $f_{-1} = f_0 - \Delta f$ and $f_1 = f_0 + \Delta f$, scale them accordingly using their received powers, and subtract them from $r_0(t)$. The resulting interference cancelled signal is

$$
\begin{aligned}
\tilde{r}_0(t) &= r_0(t) - \sqrt{P_{-1}}\, s_{-1}(t;\hat{\mathbf{b}}_{-1}) e^{-j2\pi\Delta f t} - \sqrt{P_1}\, s_1(t;\hat{\mathbf{b}}_1) e^{j2\pi\Delta f t} \\
&= \sqrt{P_0}\, s_0(t;\mathbf{b}_0) - \sqrt{P_{-1}}\, \Delta s_{-1}(t) e^{-j2\pi\Delta f t} - \sqrt{P_1}\, \Delta s_1(t) e^{j2\pi\Delta f t} + w_0(t).
\end{aligned}
\tag{6}
$$

This signal is finally sent to the demodulator in order to extract the desired bit-stream. The smaller the power of $\Delta s_{-1}(t)$ and $\Delta s_1(t)$, the better the interference are cancelled. In fact, if $\hat{\mathbf{b}}_{-1} = \mathbf{b}_{-1}$ and $\hat{\mathbf{b}}_1 = \mathbf{b}_1$ and the powers P_{-1} and P_1 are known exactly, then, ideally speaking,

the interference would be totally cancelled. We will see in the *Simulation Results* section up to what extent of system parameters, our proposed technique can function satisfactorily.

So far, we assumed that we have measured the received powers correctly. However, in practice, they must be estimated. In the next section, we propose a received power estimation technique for our interference cancellation scheme.

POWER ESTIMATION

The correct estimation of the received powers of the two adjacent channels is essential for successful *Interference Cancellation*. We perform this estimation based on the linear accumulation of powers of component signals in forming the resultant signal power. The total received power over a specific frequency band is the sum of powers contributed by the desired signal, the adjacent channel signals and the additive white noise. If we can identify these component powers, we can have an estimation of the individual received powers of the carriers. From our received signal, we can get a measure of the total power contained in a band by filtering the sequence with an appropriate filter and computing the variance of the filtered sequence. A discrete-time filter is used since the subsequent processing will be in the digital domain. Considering the complexity of brick-wall filters, we choose to use Kaiser Window [12]. The receiver will need to know values of some constants beforehand, which are defined as follows, and demonstrated in Figure 3.

A Kaiser window with fixed parameters filters an FQPSK modulated baseband signal of unit power. The variance of the resultant sequence, which we denote as x_0, gives a measure of the power in the region contained by the window [see the shaded region in Figure 3(a)]. Note that x_0 is independent of the bit sequence, and depends only on the window parameters, the carrier spacing and the bit-rate of the modulating signal. Therefore, for a given application where the bit-rate and carrier spacing are fixed, a specific Kaiser window will have a corresponding constant value of x_0. Now we shift the signal by Δf, filter it with the same window and compute the variance [see Figure 3(b)]. The resulting value x_1 is a constant as well. Shifting the signal by $-\Delta f$ [See Figure 3(c)] and performing the same yields x_{-1}. It is easy to see that $x_{-1} = x_1$. The third constant we need is a measure of the additive noise captured by the window; x_N is derived similarly after filtering a unit power AWGN [see Figure 3(d)].

We demonstrate through Figure 3(e), the linear addition of these constants weighted by received powers. Signals $s_{-1}(t)$, $s_0(t)$, and $s_1(t)$ are received at center frequencies $f_{-1} = f_0 - \Delta f$, f_0, and $f_1 = f_0 + \Delta f$, respectively, with powers P_{-1}, P_0, and P_1, respectively. The power spectral density of the additive noise is N_0. The spectra of the individual signals are shown along with their resultant sum in Figure 3(e). When a demodulator is tuned to f_0, the Kaiser window captures the region shown shaded. $S_0(f)$, centered at f_0, contributes a power of $P_0 x_0$. $S_{-1}(f)$, centered at $f_{-1} = f_0 - \Delta f$, contributes $P_{-1} x_{-1}$ while $S_1(f)$, centered at $f_1 = f_0 + \Delta f$, contributes $P_1 x_1$. Finally, the noise contributes $N_0 x_N$. Thus, the total measured power at the output of the Kaiser window is:

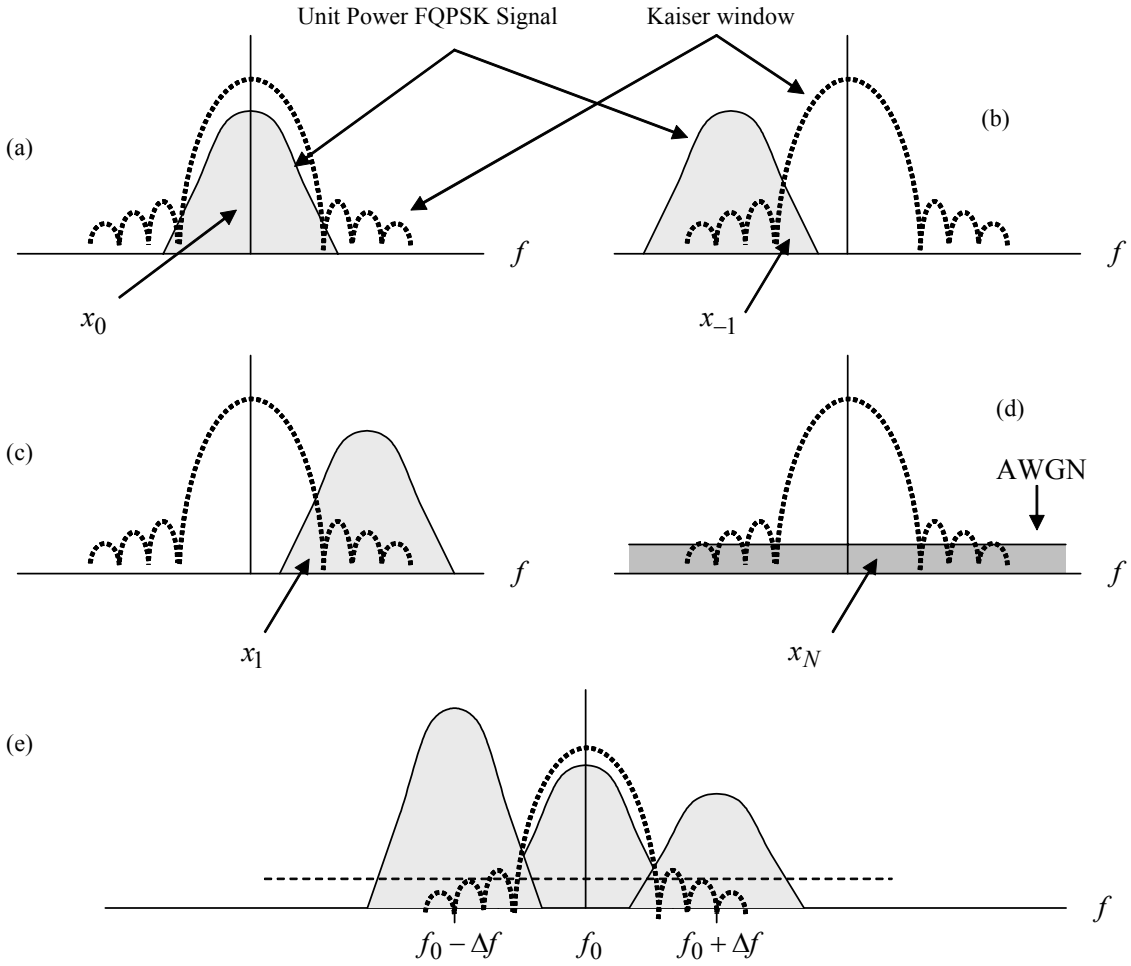

Figure 3: Illustration of power measurement using the Kaiser window.

$$P_{0X} = P_0 x_0 + P_{-1} x_1 + P_1 x_1 + N_0 x_N \tag{7}$$

Now, we put two more demodulators at the two adjacent channels tuned at $f_{-1} = f_0 - \Delta f$ and $f_1 = f_0 + \Delta f$ and perform the same. The powers at the outputs of these two Kaiser windows are

$$\begin{aligned} P_{-1X} &= P_{-1} x_0 + P_{-2} x_1 + P_0 x_1 + N_0 x_N \\ P_{1X} &= P_1 x_0 + P_0 x_1 + P_2 x_1 + N_0 x_N \end{aligned} \tag{8}$$

The values P_{-1X}, P_{0X}, and P_{1X} will be measured from the 3 receive signals, and the values x_0, x_1, and x_N are constants known at the receiver. Although, P_{-1} and P_1 are the only values we are interested in, Equations (7) – (8) actually contain a total of 6 unknowns: P_{-2}, P_{-1}, P_0, P_1, P_2, and N_0.We employ a second set of Kaiser windows with parameters different than the first Kaiser window and compute the output powers y_0, y_1, and y_N (these correspond to x_0,

x_1, and x_N with the first Kaiser window). The received signal is filtered with this new Kaiser window and its frequency-shifted versions to produce the values P_{-1Y}, P_{0Y}, and P_{1Y} given by

$$\begin{aligned} P_{-1Y} &= P_{-1}y_0 + P_{-2}y_1 + P_0 y_1 + N_0 y_N \\ P_{0Y} &= P_0 y_0 + P_{-1}y_1 + P_1 y_1 + N_0 y_N \\ P_{1Y} &= P_1 y_0 + P_0 y_1 + P_2 y_1 + N_0 y_N \end{aligned} \tag{9}$$

These measurements produce three more equations in the 6 unknowns P_{-2}, P_{-1}, P_0, P_1, P_2, and N_0. These 6 equations (7) – (9) may be expressed in matrix form as

$$\begin{bmatrix} P_{0X} \\ P_{0Y} \\ P_{-1X} \\ P_{-1Y} \\ P_{1X} \\ P_{1Y} \end{bmatrix} = \begin{bmatrix} 0 & x_1 & x_0 & x_1 & 0 & x_N \\ 0 & y_1 & y_0 & y_1 & 0 & y_N \\ x_1 & x_0 & x_1 & 0 & 0 & x_N \\ y_1 & y_0 & y_1 & 0 & 0 & y_N \\ 0 & 0 & x_1 & x_0 & x_1 & x_N \\ 0 & 0 & y_1 & y_0 & y_1 & y_N \end{bmatrix} \begin{bmatrix} P_{-2} \\ P_{-1} \\ P_0 \\ P_1 \\ P_2 \\ N_0 \end{bmatrix} \tag{10}$$

which is of the form $\mathbf{P}_w = \mathbf{KP}$. Solving for the power vector **P** gives

$$\mathbf{P} = \mathbf{K}^{-1}\mathbf{P}_w \tag{11}$$

The values in **K** will depend on the parameters of the two windows, and on the frequency spacing of the carriers. Therefore, for a given system where the separation is known, we can construct two windows and pre-calculate **K**.

A point worth mentioning here is that neither the orientation of the windows (two each at three carrier frequencies), the choice of Kaiser window as the filter, nor the parameters of the ones that we used in our simulation are optimized. We chose the size of the windows rather based on inspection of the spectra. Optimum design of the windows, or their orientation, is an important area for further research.

A few words on implementation issues: In real-time the received powers of different carriers can change quite rapidly. To precisely estimate the instantaneous powers, the received sequence over a time period (say, Δt) has to be stored first; then after the estimation process is complete, the interference cancellation and decoding can be carried on. This will increase the latency of the system, added to the computational delay due to the digital signal processing. The latency can be reduced if we approximate the powers of the signals received over (t, $t + \Delta t$) based on the variances measured over ($t - \Delta t$, t). Therefore, if over two consecutive periods of Δt, the powers are reasonably same, we do not have to hold back any signal for variance computation, but we will store them for use in the next time slot.

SIMULATION RESULTS

We performed computer simulations for the case where an FQPSK modulated signal is interfered by two other FQPSK signals, one on each side of the spectrum. We varied the signal-to-noise ratio (SNR) and the spacing between adjacent carriers and our performance metric was Bit Error Performance (BEP). For simulation in baseband, a 1 MHz carrier spacing for a 1 Mbps bit rate

yields the same results as 5 MHz spacing for 5 Mbps bit rate. Therefore, the ratio *MHz Spacing to Mbps Bit-rate* is what actually matters; we varied that from 1.0 to 0.4.

Figures 4 and 5 show the BEP vs. SNR results for an Interference-to-Carrier (I/C) ratio of 20 dB for one adjacent carrier and 0 dB for the other. With a carrier spacing of 1 MHz per 1 Mbps bit rate (see Figure 4), ACI causes about a 1 dB or lower degradation as compared to the *ACI-free* performance. It can also be seen that the performance of the proposed *Interference Cancellation technique*, however, quite closely approximates that of *ACI-free scenario*. For a highly dense spacing of 0.5 MHz per 1 Mbps (see Figure 5), ACI causes severe degradation and the BEP is quite unacceptable. Interestingly, our scheme lags the *ACI-free scenario* only by 1 - 1.5 dB.

In Figures 6 and 7, for two values of SNR (8 dB and 13 dB), we vary the frequency spacing to identify the limits of our scheme. With 8 dB SNR, the BEP starts degrading sharply only below 0.5 MHz/Mbps (see Figure 6) and with a higher SNR of 13 dB (see Figure 7) the BEP keeps in close proximity with the *ACI-free scenario* performance above a 0.6 MHz/Mbps spacing. In both cases, the ACI degradation without any *Interference Cancellation* scheme starts getting drastic right below 1.0 MHz carrier spacing.

It has been shown in [8]-[10] that for a FQPSK-B modulated signal, a minimum *frequency spacing to bit rate ratio* of about 1 is required to maintain the BEP performance in an acceptable range. Our simulations also suggest the same. With our *Interference Cancellation* scheme employed, the carrier spacing can be brought down to as low as 0.6 while maintaining less than 10^{-5} BEP. This suggests a 67% capacity increase. For a lesser stringent BEP requirement in the vicinity of 10^{-3}, our scheme can allow bringing down the carrier spacing to 0.5 MHz/Mbps, thereby suggesting a 100% capacity increase.

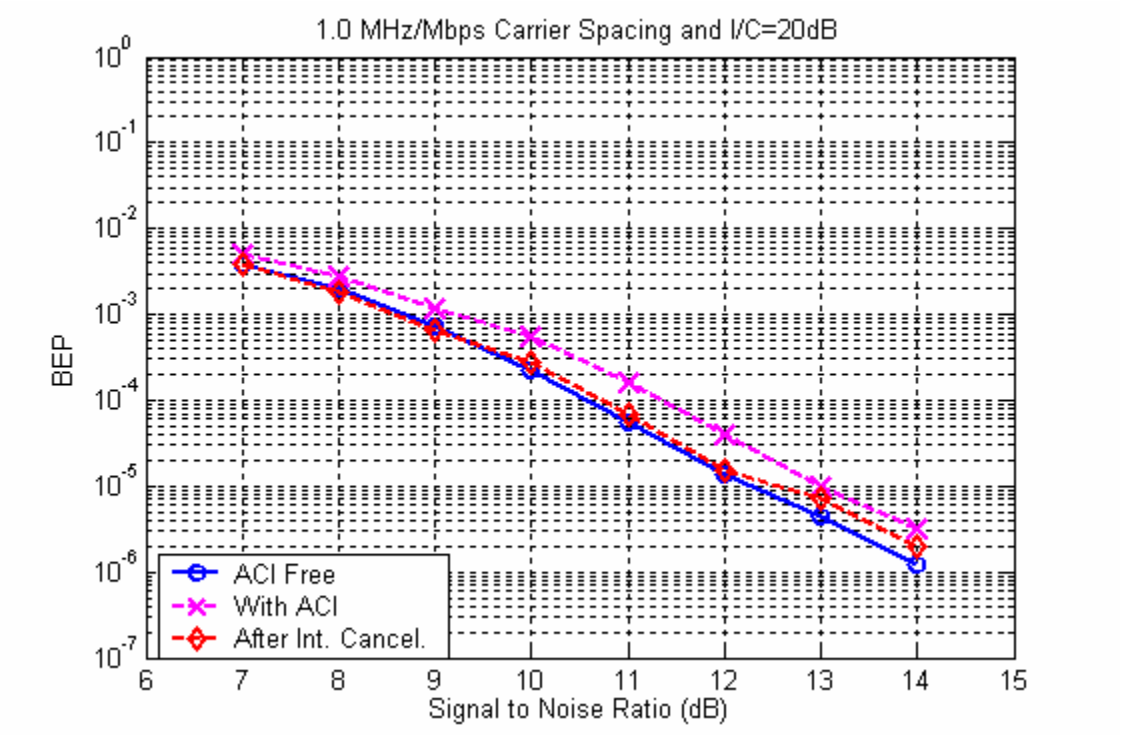

Figure 4: BEP results for 1.0 MHz/Mbps Carrier Spacing and I/C=20dB

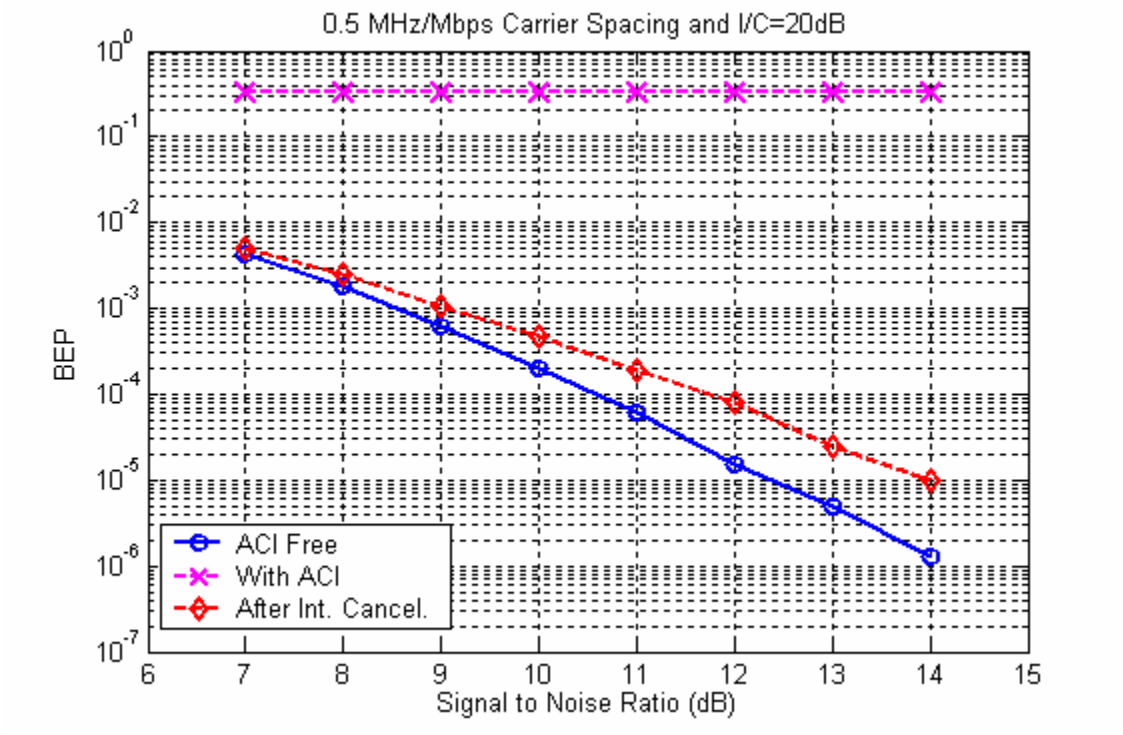

Figure 5: BEP results for 0.5 MHz/Mbps Carrier Spacing and I/C=20dB

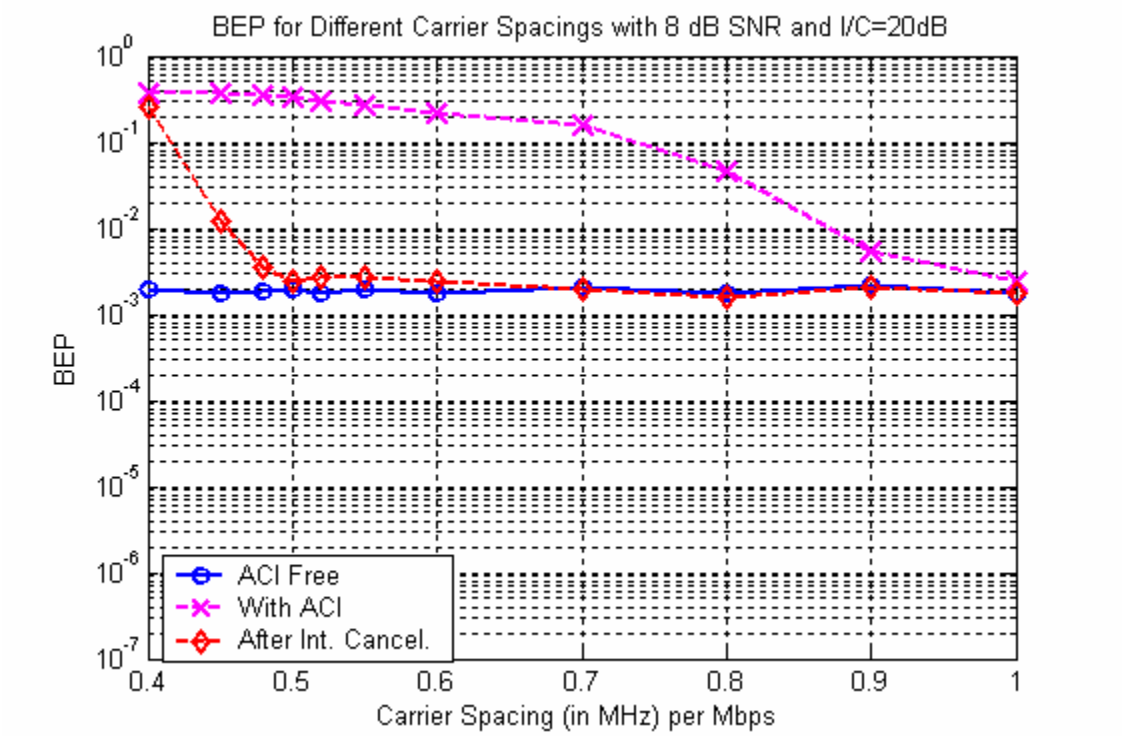

Figure 6: BEP results for different Carrier Spacings with 8 dB SNR and I/C=20dB

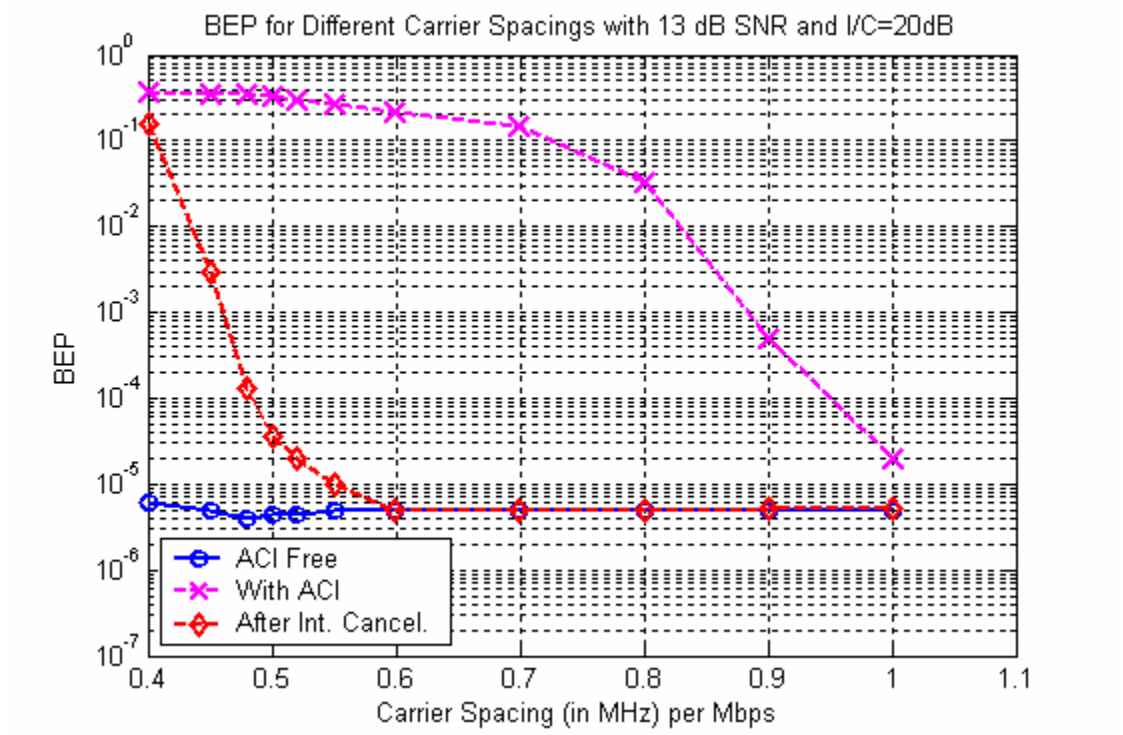

Figure 7: BEP results for different Carrier Spacings with 13 dB SNR and I/C=20dB

CONCLUSIONS

In this paper, we proposed an *Interference Cancellation technique* to suppress Adjacent Channel Interference using ARTM Tier-1 Waveforms. Our numerical study shows that for 1 Mbps bit rate signal, a carrier spacing of 0.5 ~ 0.6 MHz is achievable while existing receivers can not allow it to be below 1 MHz. This suggests a capacity increase of 100% ~ 67%. We developed our scheme for equally spaced FQPSK-B signals, but the same principle can be implemented for other modulation schemes. Even if different modulation schemes are employed in different channels and the carrier spacing is not uniform, this scheme can be implemented as long as we have knowledge of the modulation scheme(s) and the frequency spacing.

REFERENCES

[1] T. Chalfant and C. Irving, "Range Telemetry Improvement and Modernization," in Proceedings of the International Telemetering Conference, Las Vegas, NV, October 1997.

[2] W. Gao and K. Feher, "FQPSK: A Bandwidth and RF Power Efficient Technology for Telemetry Applications," in Proceedings of the International Telemetering Conference, Las Vegas, NV, October 1997.

[3] T. Hill, "An Enhanced Constant Envelope, Interoperable Shaped Offset QPSK (SOQPSK) Waveform for Improved Spectral Efficiency," in Proceedings of the International Telemetering Conference, San Diego, CA, October 2000.

[4] R. Jefferis, "FQPSK-B Baseband Filter Alternatives," in Proceedings of the International Telemetering Conference, San Diego, CA, October 2002.

[5] R. Jefferis, "Evaluation of Constant Envelope Offset Quadrature Phase Shift Keying Transmitters With a Software Based Signal Analyzer," in Proceedings of the International Telemetering Conference, San Diego, CA, October 2004.

[6] E. Law and K. Feher, "FQPSK versus PCM/FM for Aeronautical Telemetry Applications; Spectral Occupancy and Bit Error Probability Comparisons, in Proceedings of the International Telemetering Conference, Las Vegas, NV, October 1997.

[7] K. Feher, R. Jefferis, and E. Law, "Spectral Efficiency and Adjacent Channel Interference Performance Definitions and Requirements for Telemetry Applications," in Proceedings of the International Telemetering Conference, Las Vegas, NV, October 1999.

[8] E. Law, "Adjacent Channel Interference Measurements with CPFSK and FQPSK-B Signals," in Proceedings of the International Telemetering Conference, Las Vegas, NV, October 2001.

[9] E. Law, "Adjacent Channel Interference Measurements with CPFSK, CPM, and FQPSK-B Signals," in Proceedings of the International Telemetering Conference, San Diego, CA, October 2002.

[10] E. Law, "Recommended Minimum Telemetry Frequency Spacing with CPAFASK, CPM< SOQ:SK, and FQPSK Signals," in Proceedings of the International Telemetering Conference, Las Vegas, NV, October 2003.

[11] M. Haghdad and K. Feher, "Performance of FQPSK Transceivers in a Complex Real-Life Interference Environment," in Proceedings of the International Telemetering Conference, San Diego, CA, October 2000.

[12] A. Oppenheim and R. Schafer, Discrete-Time Signal Processing, second edition. Prentice Hall, 1999.